DIFFRACTION BY A HALF-PLANE IN A MOVING FLUID

P G BARTON AND A D RAWLINS

Abstract. In the following work we solve the problem of the diffraction of a plane sound wave by an impedance half plane in a moving fluid. Expressions for the total far-field are derived for both the leading edge and trailing edge situations. In the trailing edge situation the problem has the added complication of a trailing vortex sheet or wake. Hence a Kutta-Joukowski edge condition is imposed to ensure that the fluid velocity is finite at the edge and to obtain a unique solution to the problem.

1. Introduction

The problem examined in this paper is that of an insonified half-plane immersed in a moving fluid. The total far-field is derived for both the leading edge and the trailing edge situations. In the trailing edge situation the problem has the added complication of a trailing vortex sheet or wake. Hence the Kutta-Joukowski edge condition is imposed to ensure that the fluid velocity is finite at the edge and to obtain a unique solution to the problem.

As in the problem of a half plane with no flow, Barton and Rawlins [1], in the case where the impedance parameters are such that the half-plane is absorbent, the determinant of the matrix kernel is non-zero. Rawlins [2] obtained explicit expressions for the diffracted and geometrical acoustic field for the diffraction of cylindrical waves from a line source by an absorbing half-plane in the presence of a subsonic flow. However, for wave bearing surfaces, where the impedance parameter can be purely imaginary, the determinant of the matrix kernel has zeros in the cut plane. The solution given here generalizes the Wiener-Hopf-Hilbert(WWH) approach Rawlins [3], Hurd [4],Rawlins [5] to deal with both wave-bearing and non-wave-bearing surfaces in the presence of fluid flow, and allows different impedance parameters on the upper and lower surfaces of the half-plane.

In Section 2 the mathematical boundary value problem is formulated using a generalized boundary condition that arises from the combination of fluid flow and absorbent surfaces. We should remark that the boundary condition we choose to use is that of the continuity of velocity. This is not the only boundary condition that we could use. The matter of the boundary condition is still not fully resolved. Our use of this boundary condition was based on the comprehensive work of Nayfeh et al [6]. In this impressive work it is made clear (see page 134 section D, and page 144 section iv-C) that although the continuity of particle displacement is appropriate in the inviscid case on purely theoretical grounds, experimental evidence, and the lack of knowledge of the behaviour of the acoustic boundary layer would indicate that

Date: November 16, 2004 and, in revised form, November16 ,2004 .
1991 *Mathematics Subject Classification.* Primary 47A15; Secondary 46A32, 47D20.
Key words and phrases. Noise, Diffraction, Wave Scattering,aeroacoustics,half-plane.

the continuity of velocity, which is appropriate in the real fluid situation of viscosity being present, cannot be dismissed as wholly inappropriate. Also for a rigid surface with pores that allow attenuation but insignificant deformation, as with perforated steel for example, this boundary condition would be valid. Thus the boundary condition of the continuity of velocity[1] at the fluid-impedance boundary is used. The problem is then reduced to a pair of simultaneous Wiener-Hopf equations in Section 3. An explicit factorisation of the Wiener-Hopf kernel is carried out in Section 4. In Section 5 asymptotic approximations for the far-field are obtained; and the Kutta-Joukowski edge condition is imposed in section 6. Graphical plots of the modulus of the velocity potential for various values of the impedance and fluid flow parameters are given in Section 7. In the particular case of a still fluid, and the case where the admittances of the upper and lower faces of the half-plane are equal, it is shown that the results agree with Rawlins [2]. Conclusions are drawn in Section 8. Various appendices that give details of calculations of results that have been used in the main body of the paper are included at the end of the work.

2. Formulation of the Boundary Value Problem

Considered a small amplitude plane wave incident on a half-plane in a moving fluid occupying the region $x \geq 0,\ y = 0$ (see Figure1). The form of the plane wave in the moving fluid is produced by considering a line source at (x_0, y_0) that radiates cylindrical waves in a still medium. The line produced through the two points $(0,0)$ and (x_0, y_0) makes an angle θ_0 with the real positive axis on which the half-plane lies. The line source is now removed to infinity, i.e. $x_0^2 + y_0^2 \to \infty$, with the angle θ_0 remaining fixed. Apart from a constant factor, that can be set to unity, the half-plane is insonified by a unit amplitude plane wave. A wake occupies $y = 0, x < 0$ with the velocity of the moving fluid parallel to the x-axes and of magnitude $U(> 0)$. The equations of motion motion are linearised and the influence of viscosity, thermal conductivity and gravity is neglected. The fluid is assumed to have constant density and sound speed c.

The perturbation velocity $\mathbf{u}$ of the irrotational sound wave can be expressed in terms of the velocity potential $\psi(x, y, t)$ by $\mathbf{u} = \nabla\psi(x, y, t)$. The resulting pressure in the sound field is given by $p(x, y, t) = -\rho_0(\partial/\partial t + U\partial/\partial x)\psi(x, y, t)$, where ρ_0 is the density of the undisturbed stream. The velocity potential therefore satisfies the convective wave equation

$$\frac{\partial^2\psi}{\partial x^2} + \frac{\partial^2\psi}{\partial y^2} - \left(\frac{1}{c}\frac{\partial}{\partial t} - M\frac{\partial}{\partial x}\right)^2 \psi = 0,$$

where the Mach number $M = U/c$.

If a time harmonic variation $\psi(x, y, t) = \mathrm{Re}\{\psi(x, y)e^{-i\omega t}\}$ is assumed, and suppressed henceforth, the problem is one of solving the convective wave equation

$$(1 - M^2)\frac{\partial^2\psi}{\partial x^2} + \frac{\partial^2\psi}{\partial y^2} - 2ikM\frac{\partial\psi}{\partial x} + k^2\psi = 0, \tag{1}$$

with the wave number $k = \omega/c$, in all space. The half-plane surfaces are lined with materials such that β_1 and β_2 are the complex specific admittances of the upper and lower surfaces of the half-plane respectively. It is noted that for $\mathrm{Re}\ \beta_{1,2} > 0$ the

[1]It is intended to consider the alternative boundary condition of the continuity of particle dislacement in a future publication.

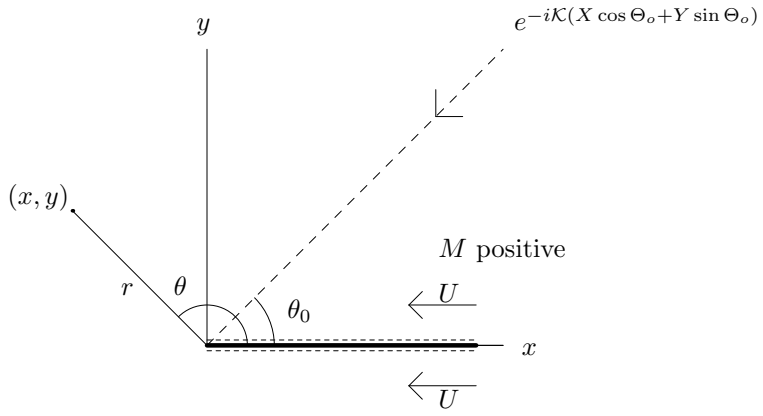

FIGURE 1. A plane wave incident on a half-plane in a moving fluid.

surface is absorbent. For Re $\beta_{1,2} = 0$ the surface no longer absorbs energy and can support surface waves provided $\beta_{1,2} = -iX_{1,2}, X_{1,2} > 0$. Therefore the boundary conditions are given by

$$\left(\frac{\partial}{\partial y} + \beta_1 M\frac{\partial}{\partial x} + ik\beta_1\right)\psi(x,0^+) = 0, \quad x > 0, \tag{2}$$

$$\left(\frac{\partial}{\partial y} - \beta_2 M\frac{\partial}{\partial x} - ik\beta_2\right)\psi(x,0^-) = 0, \quad x > 0, \tag{3}$$

$$\psi(x,0^+) - \psi(x,0^-) = 2\pi i C\exp(-ikx/M), \quad x < 0, \tag{4}$$

$$\frac{\partial\psi}{\partial y}(x,0^+) = \frac{\partial\psi}{\partial y}(x,0^-), \quad x < 0. \tag{5}$$

The boundary conditions (2) and (3) are appropriate for the continuity of velocity on the absorbent surfaces. A factor of $2\pi i$ has been introduced to the wake condition given by equation (4) to simplify formulae later on in the solution. The new constant C in this formula will be determined by the requirement that the velocity at the trailing edge should be finite. This requires the imposition of the Kutta-Joukowski edge condition. Initially, we shall impose the edge condition

$$\psi = O(1), \quad \frac{\partial\psi}{\partial y} = O(x^{-1/2}), \quad \text{as } x \to 0. \tag{6}$$

Combined with the condition that the diffracted field is outgoing at infinity. The imposition of the Kutta condition for finite velocity at the trailing edge determines the value of the constant C, and hence the unique solution of the boundary value problem. In the absence of the wake in the leading edge situation we simply set $C = 0$.

3. Solution of the Boundary Value Problem

In the presence of subsonic flow ($-1 < M < 1$) the following real substitutions can be made

$$x = \sqrt{1-M^2}X, \quad y = Y, \quad k = \sqrt{1-M^2}\,\mathcal{K}, \quad \beta = \sqrt{1-M^2}\,\mathcal{B};$$

which together with

$$\psi(x,y) = \Psi(X,Y)e^{i\mathcal{K}MX}, \tag{7}$$

reduces the problem to

$$\frac{\partial^2\Psi}{\partial X^2} + \frac{\partial^2\Psi}{\partial Y^2} + \mathcal{K}^2\Psi = 0, \tag{8}$$

subject to the boundary conditions

$$\left(\frac{\partial}{\partial Y} + \mathcal{B}_1 M\frac{\partial}{\partial X} + i\mathcal{K}\mathcal{B}_1\right)\Psi(X,0^+) = 0, \quad X > 0, \tag{9}$$

$$\left(\frac{\partial}{\partial Y} - \mathcal{B}_2 M\frac{\partial}{\partial X} - i\mathcal{K}\mathcal{B}_2\right)\Psi(X,0^-) = 0, \quad X > 0, \tag{10}$$

$$\Psi(X,0^+) - \Psi(X,0^-) = \quad 2\pi i C\exp(-i\mathcal{K}X/M), \quad X < 0, \tag{11}$$

$$\frac{\partial\Psi}{\partial Y}(X,0^+) - \frac{\partial\Psi}{\partial Y}(X,0^-) = \quad 0, \quad X < 0. \tag{12}$$

The incident plane wave is given by the expression $e^{-i\mathcal{K}(X\cos\Theta_o + Y\sin\Theta_o)}$, see [2] and [10]. A solution of the boundary value problem can now be written as

$$\Psi \quad = \Psi_{go} + \int_{-\infty}^{\infty} A(\alpha)e^{i(\alpha X + \kappa Y)}\,d\alpha, \quad Y > 0, \tag{13}$$

$$= \int_{-\infty}^{\infty} B(\alpha)e^{i(\alpha X - \kappa Y)}\,d\alpha, \qquad Y < 0. \tag{14}$$

The branch of $\kappa = (\mathcal{K}^2 - \alpha^2)^{1/2}$ is chosen such that $\kappa = +\mathcal{K}$ for $\alpha = 0$. For convenience it shall be assumed that Ψ_{go} consists of the incident plane wave and a reflected wave thus

$$\Psi_{go}(X,Y) = e^{-i\mathcal{K}(X\cos\Theta_o + Y\sin\Theta_o)} + Re^{-i\mathcal{K}(X\cos\Theta_o - Y\sin\Theta_o)}, \tag{15}$$

where

$$R = \left(\frac{\sin\Theta_o + \mathcal{B}_1 M\cos\Theta_o - \mathcal{B}_1}{\sin\Theta_o - \mathcal{B}_1 M\cos\Theta_o + \mathcal{B}_1}\right).$$

The last expression is obtained by substituting the expression (15) into the boundary condition (9) which is assumed to be satisfied for all $-\infty < X < \infty$. Applying the conditions (11) and (12) leads to

$$\begin{aligned} A(\alpha) - B(\alpha) &= l_1(\alpha) + \frac{\sin\Theta_o}{\pi i(\alpha + \mathcal{K}_o)(\sin\Theta_o - \mathcal{B}_1 M\cos\Theta_o + \mathcal{B}_1)} - \frac{C}{(\alpha + \mathcal{K}/M)}, \\ \kappa(A(\alpha) + B(\alpha)) &= l_2(\alpha) - \frac{\mathcal{K}\mathcal{B}_1\sin\Theta_o(1 - M\cos\Theta_o)}{\pi i(\alpha + \mathcal{K}_o)(\sin\Theta_o - \mathcal{B}_1 M\cos\Theta_o + \mathcal{B}_1)}, \end{aligned}$$

where $\alpha = -\mathcal{K}/M$ and $\alpha = -\mathcal{K}_o = -\mathcal{K}\cos\Theta_o$ lie in the lower half of the complex plane ($\tau_- = \text{Im}\ \alpha \le 0$) and $l_1(\alpha)$ and $l_2(\alpha)$ are analytic in this region. The capture of the poles at $\alpha = -\mathcal{K}_o$ and $\alpha = -\mathcal{K}/M$ is shown in Figure 2.

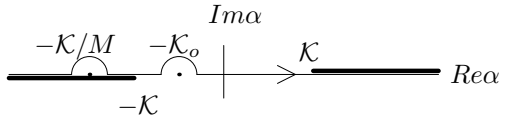

FIGURE 2. The complex plane.

By adding and subtracting these equations it can be seen that

(16)
$$A(\alpha) = \frac{1}{2}\left\{ l_1(\alpha) + \frac{l_2(\alpha)}{\kappa} - \frac{\sin\Theta_o\{\mathcal{K}\mathcal{B}_1(1 - M\cos\Theta_o)/\kappa - 1\}}{\pi i(\alpha + \mathcal{K}_o)(\sin\Theta_o - \mathcal{B}_1 M\cos\Theta_o + \mathcal{B}_1)} - \frac{C}{(\alpha + \mathcal{K}/M)} \right\},$$

(17)
$$B(\alpha) = \frac{1}{2}\left\{ -l_1(\alpha) + \frac{l_2(\alpha)}{\kappa} - \frac{\sin\Theta_o\{\mathcal{K}\mathcal{B}_1(1 - M\cos\Theta_o)/\kappa + 1\}}{\pi i(\alpha + \mathcal{K}_o)(\sin\Theta_o - \mathcal{B}_1 M\cos\Theta_o + \mathcal{B}_1)} + \frac{C}{(\alpha + \mathcal{K}/M)} \right\}.$$

Applying the boundary conditions (9) and (10) leads to

$$(\mathcal{K}\mathcal{B}_1 + \kappa + \mathcal{B}_1 M\alpha)A(\alpha) \qquad = u_1(\alpha), \tag{18}$$

$$(\mathcal{K}\mathcal{B}_2 + \kappa + \mathcal{B}_2 M\alpha)B(\alpha) \qquad = u_2(\alpha), \tag{19}$$

where $u_1(\alpha)$ and $u_2(\alpha)$ are analytic in the upper half-plane, τ_+: Im $\alpha \geq 0, \alpha \neq -\mathcal{K}_o, \alpha \neq -\mathcal{K}/M$. Substituting (16) and (17) into these equations eliminates the unknowns $A(\alpha), B(\alpha)$ and leads to the matrix Wiener-Hopf equation

$$G(\alpha)\, l(\alpha) = u(\alpha) + G(\alpha)\frac{P}{(\alpha + \mathcal{K}_o)} + \frac{G(\alpha)}{(\alpha + \mathcal{K}/M)}\begin{pmatrix} C \\ 0 \end{pmatrix}, \tag{20}$$

where

$$G(\alpha) = \frac{1}{2}\begin{pmatrix} \kappa + \mathcal{B}_1 M\alpha + \mathcal{K}\mathcal{B}_1 & (\kappa + \mathcal{B}_1 M\alpha + \mathcal{K}\mathcal{B}_1)/\kappa \\ -\kappa - \mathcal{B}_2 M\alpha - \mathcal{K}\mathcal{B}_2 & (\kappa + \mathcal{B}_2 M\alpha + \mathcal{K}\mathcal{B}_2)/\kappa \end{pmatrix}, \tag{21}$$

$$P = \frac{-\sin\Theta_o}{\pi i(\sin\Theta_o - \mathcal{B}_1 M\cos\Theta_o + \mathcal{B}_1)}\begin{pmatrix} 1 \\ -\mathcal{K}\mathcal{B}_1(1 - M\cos\Theta_o) \end{pmatrix},$$

$$l(\alpha) = \begin{pmatrix} l_1 \\ l_2 \end{pmatrix}, \quad u(\alpha) = \begin{pmatrix} u_1 \\ u_2 \end{pmatrix}.$$

The problem of factorising the matrix $G(\alpha)$ is addressed in a manner similar to that in Barton and Rawlins [1]. Firstly, define $D(\alpha)$ such that

$$D^2(\alpha) = \det G(\alpha) = \frac{1}{2\kappa}(\kappa + \mathcal{B}_1 M\alpha + \mathcal{K}\mathcal{B}_1)(\kappa + \mathcal{B}_2 M\alpha + \mathcal{K}\mathcal{B}_2),$$

and define $K(\alpha)$ by

$$G(\alpha) = D(\alpha)K(\alpha). \tag{22}$$

Then

(23)
$$K(\alpha) = \sqrt{\frac{\kappa}{2}}\begin{pmatrix} \left(\dfrac{\kappa + \mathcal{B}_1 M\alpha + \mathcal{K}\mathcal{B}_1}{\kappa + \mathcal{B}_2 M\alpha + \mathcal{K}\mathcal{B}_2}\right)^{1/2} & \dfrac{1}{\kappa}\left(\dfrac{\kappa + \mathcal{B}_1 M\alpha + \mathcal{K}\mathcal{B}_1}{\kappa + \mathcal{B}_2 M\alpha + \mathcal{K}\mathcal{B}_2}\right)^{1/2} \\ -\left(\dfrac{\kappa + \mathcal{B}_2 M\alpha + \mathcal{K}\mathcal{B}_2}{\kappa + \mathcal{B}_1 M\alpha + \mathcal{K}\mathcal{B}_1}\right)^{1/2} & \dfrac{1}{\kappa}\left(\dfrac{\kappa + \mathcal{B}_2 M\alpha + \mathcal{K}\mathcal{B}_2}{\kappa + \mathcal{B}_1 M\alpha + \mathcal{K}\mathcal{B}_1}\right)^{1/2} \end{pmatrix},$$

and

$$\det K(\alpha) = 1.$$

The factorisation of $G(\alpha)$ now follows directly from the factorisation of $K(\alpha)$ and $D(\alpha)$.

4. Factorisation of the Wiener-Hopf Kernel

Factorisation of $K(\alpha)$. It is required that $K(\alpha) = U(\alpha)L^{-1}(\alpha)$ where $L(\alpha)$ is analytic everywhere except along the line $\mathcal{K} < \alpha < \infty$, $\mathrm{Im}(\alpha) = 0$ and $U(\alpha)$ is analytic everywhere except along $-\infty < \alpha < -\mathcal{K}$, $\mathrm{Im}(\alpha) = 0$. Then it can be written that

$$\left.\begin{array}{l} K^+(\xi) = U^+(\xi)L^{-1}(\xi) \\ K^-(\xi) = U^-(\xi)L^{-1}(\xi) \end{array}\right\}, -\infty < \xi < -\mathcal{K}, \tag{24}$$

since L is continuous across this region. Eliminating $L^{-1}(\xi)$ gives

$$U^+(\xi) = K^+(\xi)[K^{-1}(\xi)]^- U^-(\xi), \tag{25}$$

where F^+ denotes values of F on the upper side of the cut and F^- denotes values of F on the lower side of the cut. From equation (23) it follows that

$$K^+(\xi) = \sqrt{\frac{i|\kappa|}{2}} \begin{pmatrix} \left(\dfrac{i|\kappa| - \mathcal{B}_1 M|\xi| + \mathcal{K}\mathcal{B}_1}{i|\kappa| - \mathcal{B}_2 M|\xi| + \mathcal{K}\mathcal{B}_2}\right)^{1/2} & \dfrac{1}{i|\kappa|}\left(\dfrac{i|\kappa| - \mathcal{B}_1 M|\xi| + \mathcal{K}\mathcal{B}_1}{i|\kappa| - \mathcal{B}_2 M|\xi| + \mathcal{K}\mathcal{B}_2}\right)^{1/2} \\ -\left(\dfrac{i|\kappa| - \mathcal{B}_2 M|\xi| + \mathcal{K}\mathcal{B}_2}{i|\kappa| - \mathcal{B}_1 M|\xi| + \mathcal{K}\mathcal{B}_1}\right)^{1/2} & \dfrac{1}{i|\kappa|}\left(\dfrac{i|\kappa| - \mathcal{B}_2 M|\xi| + \mathcal{K}\mathcal{B}_2}{i|\kappa| - \mathcal{B}_1 M|\xi| + \mathcal{K}\mathcal{B}_1}\right)^{1/2} \end{pmatrix},$$

$$[K^{-1}(\xi)]^- = \sqrt{\frac{-i|\kappa|}{2}} \begin{pmatrix} \dfrac{-1}{i|\kappa|}\left(\dfrac{-i|\kappa| - \mathcal{B}_2 M|\xi| + \mathcal{K}\mathcal{B}_2}{-i|\kappa| - \mathcal{B}_1 M|\xi| + \mathcal{K}\mathcal{B}_1}\right)^{1/2} & \dfrac{1}{i|\kappa|}\left(\dfrac{-i|\kappa| - \mathcal{B}_1 M|\xi| + \mathcal{K}\mathcal{B}_1}{-i|\kappa| - \mathcal{B}_2 M|\xi| + \mathcal{K}\mathcal{B}_2}\right)^{1/2} \\ \left(\dfrac{-i|\kappa| - \mathcal{B}_2 M|\xi| + \mathcal{K}\mathcal{B}_2}{-i|\kappa| - \mathcal{B}_1 M|\xi| + \mathcal{K}\mathcal{B}_1}\right)^{1/2} & \left(\dfrac{-i|\kappa| - \mathcal{B}_1 M|\xi| + \mathcal{K}\mathcal{B}_1}{-i|\kappa| - \mathcal{B}_2 M|\xi| + \mathcal{K}\mathcal{B}_2}\right)^{1/2} \end{pmatrix}.$$

Substituting these into equation (25) gives

$$U^+(\xi) = \begin{pmatrix} 0 & -i\left\{\frac{(\mathcal{K}\mathcal{B}_1 - \mathcal{B}_1 M|\xi|)^2 + |\kappa|^2}{(\mathcal{K}\mathcal{B}_2 - \mathcal{B}_2 M|\xi|)^2 + |\kappa|^2}\right\}^{\frac{1}{2}} \\ -i\left\{\frac{(\mathcal{K}\mathcal{B}_2 - \mathcal{B}_2 M|\xi|)^2 + |\kappa|^2}{(\mathcal{K}\mathcal{B}_1 - \mathcal{B}_1 M|\xi|)^2 + |\kappa|^2}\right\}^{\frac{1}{2}} & 0 \end{pmatrix} U^-(\xi). \tag{26}$$

This requires the solution of the following coupled Hilbert problems

$$U_1^+(\xi) = -i\left\{\frac{(\mathcal{K}\mathcal{B}_1 - \mathcal{B}_1 M|\xi|)^2 + |\kappa|^2}{(\mathcal{K}\mathcal{B}_2 - \mathcal{B}_2 M|\xi|)^2 + |\kappa|^2}\right\}^{\frac{1}{2}} U_2^-(\xi), \tag{27}$$

$$U_2^+(\xi) = -i\left\{\frac{(\mathcal{K}\mathcal{B}_2 - \mathcal{B}_2 M|\xi|)^2 + |\kappa|^2}{(\mathcal{K}\mathcal{B}_1 - \mathcal{B}_1 M|\xi|)^2 + |\kappa|^2}\right\}^{\frac{1}{2}} U_1^-(\xi). \tag{28}$$

If $V(\xi) = U_1(\xi)U_2(\xi)$ and $W(\xi) = \dfrac{U_1(\xi)}{U_2(\xi)}$ then multiplying and dividing the Hilbert equations produces

$$V^+(\xi)/V^-(\xi) = -1, \tag{29}$$

$$[\log W(\xi)]^+ + [\log W(\xi)]^- = \log\left[\frac{|\kappa|^2 + (\mathcal{K}\mathcal{B}_1 - \mathcal{B}_1 M|\xi|)^2}{|\kappa|^2 + (\mathcal{K}\mathcal{B}_2 - \mathcal{B}_2 M|\xi|)^2}\right]. \tag{30}$$

By inspection, it can be seen that equation (29) has a particular solution

$$V(\alpha) = (\mathcal{K}+\alpha)^{-\frac{1}{2}}. \tag{31}$$

Equation (30) can be written as

$$\left[\frac{\log W(\xi)}{\sqrt{\mathcal{K}+\xi}}\right]^{+} - \left[\frac{\log W(\xi)}{\sqrt{\mathcal{K}+\xi}}\right]^{-} = \frac{-i}{|\mathcal{K}+\xi|^{1/2}} \log\left[\frac{|\kappa|^2+(\mathcal{K}\mathcal{B}_1-\mathcal{B}_1 M|\xi|)^2}{|\kappa|^2+(\mathcal{K}\mathcal{B}_2-\mathcal{B}_2 M|\xi|)^2}\right]. \tag{32}$$

The solution of this equation (see Appendix A) is given by

$$W(\alpha) = \exp\left[-\frac{\sqrt{\mathcal{K}+\alpha}}{2\pi}\int_{-\infty}^{-\mathcal{K}} \frac{1}{|\mathcal{K}+t|^{\frac{1}{2}}} \log\left[\frac{|\kappa|^2+(\mathcal{K}\mathcal{B}_1-\mathcal{B}_1 M|t|)^2}{|\kappa|^2+(\mathcal{K}\mathcal{B}_2-\mathcal{B}_2 M|t|)^2}\right]\frac{dt}{(t-\alpha)}\right]. \tag{33}$$

Now,

$$\begin{aligned} I(\alpha) &= -\frac{1}{2\pi}\int_{-\infty}^{-\mathcal{K}} \frac{1}{|\mathcal{K}+t|^{\frac{1}{2}}} \log\left[\frac{|\kappa|^2+(\mathcal{K}\mathcal{B}_1-\mathcal{B}_1 M|t|)^2}{|\kappa|^2+(\mathcal{K}\mathcal{B}_2-\mathcal{B}_2 M|t|)^2}\right]\frac{dt}{(t-\alpha)}, \\ &= \frac{1}{2\pi}\int_0^{\infty} \frac{\log(t+\mathcal{K}B_1^{+}) + \log(t+\mathcal{K}B_1^{-}) - \log(t+\mathcal{K}B_2^{+}) - \log(t+\mathcal{K}B_2^{-})}{t^{\frac{1}{2}}(t+\mathcal{K}+\alpha)}\, dt \\ &\qquad + \frac{1}{2\pi}\log\left(\frac{1+\mathcal{B}_1^2M^2}{1+\mathcal{B}_2^2M^2}\right)\int_0^{\infty}\frac{dt}{t^{1/2}(t+\mathcal{K}+\alpha)}, \end{aligned}$$

where

$$B_{1,2}^{\pm} = 1 - \frac{\mathcal{B}_{1,2}^2 M \pm \sqrt{1+\mathcal{B}_{1,2}^2M^2-\mathcal{B}_{1,2}^2}}{1+\mathcal{B}_{1,2}^2M^2}. \tag{34}$$

Using the following results (see Appendix B)

$$\int_0^{\infty}\frac{\log(t+\delta)}{t^{\frac{1}{2}}(t+\gamma)}dt = \frac{2\pi}{\sqrt{\gamma}}\log(\sqrt{\gamma}+\sqrt{\delta}),\ |\arg\gamma|<\pi, |\arg\delta|\le\pi, \tag{35}$$

$$\frac{1}{2\pi}\log\left(\frac{1+\mathcal{B}_1^2M^2}{1+\mathcal{B}_2^2M^2}\right)\int_0^{\infty}\frac{dt}{t^{1/2}(t+\mathcal{K}+\alpha)} = \frac{1}{\sqrt{\mathcal{K}+\alpha}}\log\left(\frac{1+\mathcal{B}_1^2M^2}{1+\mathcal{B}_2^2M^2}\right)^{1/2},$$

equation (33) reduces to

$$W(\alpha) = \left(\frac{1+\mathcal{B}_1^2M^2}{1+\mathcal{B}_2^2M^2}\right)^{1/2}\frac{\left(\sqrt{\mathcal{K}+\alpha}+\sqrt{\mathcal{K}B_1(+)}\right)\left(\sqrt{\mathcal{K}+\alpha}+\sqrt{\mathcal{K}B_1(-)}\right)}{\left(\sqrt{\mathcal{K}+\alpha}+\sqrt{\mathcal{K}B_2(+)}\right)\left(\sqrt{\mathcal{K}+\alpha}+\sqrt{\mathcal{K}B_2(-)}\right)}. \tag{36}$$

Particular solutions of (27) and (28) are now given by

$$\begin{aligned} U_1(\alpha) &= -[V(\alpha)]^{\frac{1}{2}}[W(\alpha)]^{\frac{1}{2}}, \\ U_2(\alpha) &= -[V(\alpha)]^{\frac{1}{2}}[W(\alpha)]^{-\frac{1}{2}}. \end{aligned}$$

A general solution can be obtained by following the method given by Rawlins [5]. This is done by imposing further conditions on the functions $U_1(\alpha)$ and $U_2(\alpha)$. First it is required that

$$U_1(\alpha) = O((\mathcal{K}+\alpha)^n), \quad U_2(\alpha) = O((\mathcal{K}+\alpha)^{1/2+m}), \quad \text{as } \alpha \to -k,$$

for some $n, m > -1$. The second requirement is that $U_1(\alpha)$ and $U_2(\alpha)$ have finite degree at infinity. These conditions lead to

$$U(\alpha) = U^{(0)}(\alpha)P(\alpha),$$

where $P_{ij}(i,j=1,2)$ are arbitrary polynomials and

$$U^{(0)}(\alpha)=\begin{pmatrix} -[V(\alpha)]^{\frac{1}{2}}[W(\alpha)]^{\frac{1}{2}} & [V(\alpha)]^{\frac{1}{2}}[W(\alpha)]^{\frac{1}{2}}[\mathcal{K}+\alpha]^{\frac{1}{2}} \\ -[V(\alpha)]^{\frac{1}{2}}[W(\alpha)]^{-\frac{1}{2}} & -[V(\alpha)]^{\frac{1}{2}}[W(\alpha)]^{-\frac{1}{2}}[\mathcal{K}+\alpha]^{\frac{1}{2}} \end{pmatrix}.$$

To ensure that U is non-singular in the cut plane $\det U$ and hence $\det P$ must be non-zero for all α. The fact that $\det P$ is a polynomial implies that $\det P=$ constant. For simplicity, P is chosen to be the identity matrix. This gives a final expression of

$$U(\alpha)=\begin{pmatrix} -[\mathcal{K}+\alpha]^{-\frac{1}{4}}[W(\alpha)]^{\frac{1}{2}} & [\mathcal{K}+\alpha]^{\frac{1}{4}}[W(\alpha)]^{\frac{1}{2}} \\ -[\mathcal{K}+\alpha]^{-\frac{1}{4}}[W(\alpha)]^{-\frac{1}{2}} & -[\mathcal{K}+\alpha]^{\frac{1}{4}}[W(\alpha)]^{-\frac{1}{2}} \end{pmatrix}. \tag{37}$$

The matrix $L(\alpha)$ can be found from the expression

$$L(\alpha)=K^{-1}(\alpha)U(\alpha).$$

Factorisation of $D(\alpha)$.

$$\begin{aligned} D(\alpha) &= \sqrt{\frac{(\kappa+\mathcal{B}_1M\alpha+\mathcal{K}\mathcal{B}_1)(\kappa+\mathcal{B}_2M\alpha+\mathcal{K}\mathcal{B}_1)}{2\kappa}}, \\ &= \left(\frac{\kappa}{2}\right)^{1/2}\left(\frac{\kappa+\mathcal{B}_1M\alpha+\mathcal{K}\mathcal{B}_1}{\kappa}\right)^{1/2}\left(\frac{\kappa+\mathcal{B}_2M\alpha+\mathcal{K}\mathcal{B}_2}{\kappa}\right)^{1/2}. \end{aligned}$$

Consider the factorisation of the function $d^n(\alpha)$ given by

$$d^n(\alpha)=\frac{\kappa+\mathcal{B}_nM\alpha+\mathcal{K}\mathcal{B}_n}{\kappa}. \tag{38}$$

This function has been factorised explicitly in Rawlins [2]. The upper split function is

(39)

$$d^n_+(\mathcal{K}\cos\Theta)=\frac{\sqrt{1+\mathcal{B}_n}}{\sqrt{1+\cos\Theta}}\exp\left\{\frac{\mathcal{B}_n}{2\pi\sqrt{1-\mathcal{B}_n^2+M^2\mathcal{B}_n^2}}\Big[F(v_1)-F(v_2)\Big]\right\},\ \ 0\le\Theta<\pi,$$

where

$$F(v)=-(M+v)\int_{\pi/2}^{\Theta}\frac{u-\frac{\arccos v}{\sqrt{1-v^2}}\sin u du}{(v-\cos u)}, \tag{40}$$

and

$$v_1=\frac{-M\mathcal{B}_n^2+\sqrt{1-\mathcal{B}_n^2+M^2\mathcal{B}_n^2}}{1+\mathcal{B}_n^2M^2},\ \ v_2=\frac{-M\mathcal{B}_n^2-\sqrt{1-\mathcal{B}_n^2+M^2\mathcal{B}_n^2}}{1+\mathcal{B}_n^2M^2}. \tag{41}$$

The upper split function, $D_+(\alpha)$, can now be written as

$$D_+(\alpha)=\left\{\sqrt{\frac{\mathcal{K}+\alpha}{2}}d_1^+(\alpha)d_2^+(\alpha)\right\}^{1/2}. \tag{42}$$

5. Asymptotic Expressions for the Far-Field

With the factorisation of $G(\alpha)$ complete, the procedure from equation (20) is as follows

$$\begin{aligned} G(\alpha)l(\alpha) &= u(\alpha) + G(\alpha)\frac{P}{(\alpha+\mathcal{K}_o)} + \frac{G(\alpha)}{(\alpha+\mathcal{K}/M)}\begin{pmatrix}C\\0\end{pmatrix}, \\ G_+(\alpha)G_-(\alpha)l(\alpha) &= u(\alpha) + G(\alpha)\frac{P}{(\alpha+\mathcal{K}_o)} + \frac{G(\alpha)}{(\alpha+\mathcal{K}/M)}\begin{pmatrix}C\\0\end{pmatrix}, \\ G_-(\alpha)l(\alpha) &= G_+^{-1}(\alpha)u(\alpha) + G_-(\alpha)\frac{P}{(\alpha+\mathcal{K}_o)} + \frac{G_-(\alpha)}{(\alpha+\mathcal{K}/M)}\begin{pmatrix}C\\0\end{pmatrix}. \end{aligned}$$

This can be written in the form

(43)
$$\begin{aligned} G_-(\alpha)l(\alpha) - \Big[G_-(\alpha) - G_-(-\mathcal{K}_o)\Big]\frac{P}{(\alpha+\mathcal{K}_o)} - \frac{[G_-(\alpha) - G_-(-\mathcal{K}/M)]}{(\alpha+\mathcal{K}/M)}\begin{pmatrix}C\\0\end{pmatrix} \\ = G_+^{-1}(\alpha)u(\alpha) + G_-(-\mathcal{K}_o)\frac{P}{(\alpha+\mathcal{K}_o)} + \frac{G_-(-\mathcal{K}/M)}{(\alpha+\mathcal{K}/M)}\begin{pmatrix}C\\0\end{pmatrix}. \end{aligned}$$

The left hand side of this expression is analytic in τ_- and the right hand side is analytic in τ_+. Hence both sides of equation (43) are equal to an entire function $\mathbf{Q}(\alpha)$. From equations (31) and (36) it follows that

$$V(\alpha) = O(\alpha^{-\frac{1}{2}}), \quad W(\alpha) = O(1), \quad |\alpha| \to \infty.$$

Therefore

$$G_+(\alpha) = O\begin{pmatrix}1 & \alpha^{\frac{1}{2}}\\ 1 & \alpha^{\frac{1}{2}}\end{pmatrix}, \quad G_-(\alpha) = O\begin{pmatrix}\alpha^{-\frac{1}{2}} & 1\\ \alpha^{\frac{1}{2}} & \alpha^{-1}\end{pmatrix}, \quad |\alpha| \to \infty. \tag{44}$$

Combining the edge condition (6) with (18) it can be shown that the terms of $u(\alpha)$ are $\mathrm{O}(\alpha^{-1/2})$ at worst. Using an extension of Liouville's theorem it now follows that $\mathbf{Q}(\alpha) = 0$. Thus

$$\begin{aligned} l(\alpha) &= -\frac{\left[G_-^{-1}(\alpha)\, G_-(-\mathcal{K}/M) - \mathrm{I}\right]}{(\alpha+\mathcal{K}/M)}\begin{pmatrix}C\\0\end{pmatrix} \\ &\quad - \left[G_-^{-1}(\alpha)G_-(-\mathcal{K}_o) - \mathrm{I}\right]\frac{P}{(\alpha+\mathcal{K}_o)}, \end{aligned} \tag{45}$$

$$u(\alpha) = -\frac{G_+(\alpha)\, G_-(-\mathcal{K}/M)}{(\alpha+\mathcal{K}/M)}\begin{pmatrix}C\\0\end{pmatrix} - G_+(\alpha)G_-(-\mathcal{K}_o)\frac{P}{(\alpha+\mathcal{K}_o)}. \tag{46}$$

Combining (46) with (13) and (18) gives

(47)
$$\Psi(X,Y) - \Psi_{go}(X,Y) = \Psi_s(X,Y) = \int_{-\infty}^{\infty} \frac{u_1(\alpha)}{(\kappa + \mathcal{B}_1 M\alpha + \mathcal{K}\mathcal{B}_1)}\, e^{i(\alpha X + \kappa Y)}d\alpha, \quad y > 0.$$

Similarly by using (46) with (24) and (29) gives,

$$\Psi(X,Y) = \int_{-\infty}^{\infty} \frac{u_2(\alpha)}{(\kappa + \mathcal{B}_2 M\alpha + \mathcal{K}\mathcal{B}_2)}\, e^{i(\alpha X - \kappa Y)}d\alpha, \quad y < 0. \tag{48}$$

As was seen in Barton and Rawlins [1], the procedure from here is to consider a shift of contour in the α-plane given by

$$\alpha = \mathcal{K}\cos(\Theta + it), \quad (-\infty < t < \infty). \tag{49}$$

On applying this to equation (47), the scattered field becomes

$$\Psi_s(R,\Theta) = \int_{-\infty}^{\infty} \frac{-i\sin(\Theta+it)\; u_1[\mathcal{K}\cos(\Theta+it)]}{\mathcal{B}_1+\mathcal{B}_1 M\cos(\Theta+it)+\sin(\Theta+it)} e^{i\mathcal{K}R\cosh t}dt, \quad 0<\Theta<\pi. \tag{50}$$

A similar appropriate representation for $\Psi(X,Y)$ in $y<0$ can be obtained. On applying the method of stationary phase, the final expression for the far-field is

$$\Psi(R,\Theta) = \Psi_i(R,\Theta)+\Psi_r(R,\Theta)+\Psi_{d+}(R,\Theta), \qquad 0<\Theta<\pi-\Theta_o, \tag{51}$$

$$= \Psi_i(R,\Theta)+\Psi_{d+}(R,\Theta), \qquad \pi-\Theta_o<\Theta<\pi, \tag{52}$$

$$= \Psi_i(R,\Theta)+\Psi_{d-}(R,\Theta), \qquad -\pi<\Theta<\Theta_o-\pi, \tag{53}$$

$$= \Psi_{d-}(R,\Theta), \qquad \Theta_o-\pi<\Theta<0, \tag{54}$$

where

$$\Psi_i(R,\Theta) = e^{-i\mathcal{K}R\cos(\Theta-\Theta_o)}, \tag{55}$$

$$\Psi_r(R,\Theta) = \left(\frac{\sin\Theta_o+\mathcal{B}_1 M\cos\Theta_o-\mathcal{B}_1}{\sin\Theta_o-\mathcal{B}_1 M\cos\Theta_o+\mathcal{B}_1}\right)e^{-i\mathcal{K}R\cos(\Theta+\Theta_o)}, \tag{56}$$

$$\Psi_{d_+}(R,\Theta) = 2i\sqrt{\frac{\pi}{2\mathcal{K}R}}\left(\frac{\sin\Theta}{\mathcal{B}_1+\mathcal{B}_1 M\cos\Theta+\sin\Theta}\right)u_1[\mathcal{K}\cos\Theta]e^{i\mathcal{K}R+\frac{\pi i}{4}}, \tag{57}$$

$$\Psi_{d_-}(R,\Theta) = -2i\sqrt{\frac{\pi}{2\mathcal{K}R}}\left(\frac{\sin\Theta}{\mathcal{B}_2+\mathcal{B}_2 M\cos\Theta-\sin\Theta}\right)u_2[\mathcal{K}\cos\Theta]e^{i\mathcal{K}R+\frac{\pi i}{4}}, \tag{58}$$

and

$$\sin\Theta = \frac{\sin\theta(1-M^2)^{1/2}}{(1-M^2\sin^2\theta)^{1/2}}, \quad \cos\Theta = \frac{\cos\theta}{(1-M^2\sin^2\theta)^{1/2}}, \quad R = r\left(\frac{1-M^2\sin^2\theta}{1-M^2}\right)^{1/2}.$$

6. The Kutta-Joukowski Condition

In the trailing edge situation ($M>0$) the unknown C is calculated by applying the Kutta-Joukowski edge condition. In the absence of a wake $C=0$. The Kutta-Joukowski condition requires that the velocity be finite at the origin which means that the terms in $\frac{\partial\Psi}{\partial y}$ that are $O(r^{-1/2})$ must vanish or terms of Ψ that are $O(r^{1/2})$. This in turn implies that the terms of $O(\alpha^{-1/2})$ in $u_1(\alpha)$ and $u_2(\alpha)$ must also vanish. From expression (46) it can be seen that

$$u_1(\alpha) = -\frac{C\{G_1(\alpha)e+G_2(\alpha)g\}}{(\alpha+\mathcal{K}/M)} - \frac{1}{(\alpha+\mathcal{K}_o)}\Big[G_1(\alpha)\{aP_1+bP_2\}+G_2(\alpha)\{cP_1+dP_2\}\Big],$$

where

$$G_+(\alpha) = \begin{pmatrix} G_1(\alpha) & G_2(\alpha) \\ G_3(\alpha) & G_4(\alpha)\end{pmatrix}, \; G_-(-\mathcal{K}_o) = \begin{pmatrix} a & b \\ c & d\end{pmatrix}, \; G_-(-\mathcal{K}/M) = \begin{pmatrix} e & f \\ g & h\end{pmatrix},$$

$$P = \begin{pmatrix} P_1 \\ P_2\end{pmatrix}.$$

From (44) it can be seen that G_1 and G_3 are $O(1)$ whilst G_2 and G_4 are $O(\alpha^{1/2})$ as $|\alpha|\to\infty$. Setting the term that is $O(\alpha^{-1/2})$ to zero in $u_1(\alpha)$ gives

$$cP_1+dP_2+gC=0,$$

$$C = -\frac{(cP_1+dP_2)}{g}. \tag{59}$$

7. Graphical Results

The modulus of the velocity potential function is proportional to the amplitude of the perturbation sound pressure; and therefore gives a measure of sound intensity. Graphical plots of the modulus of the velocity potential function, given by the far field expressions (55) to (58) for ($kr = 10\pi$), are shown in the following graphs where the angle of incidence is taken to be $\pi/2$, the Mach number, M, takes the values -0.9, 0, and 0.9 and the impedance parameters take various values . In the trailing edge situation ($M > 0$) graphs have been obtained in the case where a wake is present and, in the leading edge situation ($M \leq 0$) where no wake is present($C = 0$). The diffracted field given by expressions (57) and (58) becomes infinite on the boundaries $\Theta = \pi - \Theta_o$ and $\Theta = \pi + \Theta_o$ so a uniform asymptotic expression has been used to give the graphical plots of the modulus of the far-field. See Appendix C for further details.

As a check on the analysis and coding for graphical results the graphs obtained in Rawlins [2] for $\beta_1 = \beta_2 = 2/3$ (fibrous sheet) and $\beta_1 = \beta_2 = 1/(0.5 + i)$(perforated steel) were reproduced and found to be identical, except the figure 2 and 4 in Rawlins [2], which should be transposed. The typical type of graph obtained for impedances being the same on both faces of the half-plane are shown in figures 3-5. These show the modulus of the far-field for a half-plane with impedance parameter $\beta_1 = \beta_2 = 0.5 - i$. The polar plot for $M = 0$ is not shown since it is identical with that of figure 7 of Barton and Rawlins [1]. The field in the region $0 < \theta < \pi/2$ is due primarily to interference between the incident and reflected wave. The modulus of the reflection coefficient is given by expression (56) and is $|\Psi_r| \simeq 0.7$ for $M = \pm 0.9$.

It can be seen that in the region $0 < \theta < \frac{1}{2}\pi$ the oscillations about the incident wave magnitude of unity are of order$|\Psi_r|$. The frequency of the oscillations increases with $|M|, -1 < M < 1$. These graphs differ, but not significantly, in the region $\frac{1}{2}\pi < \theta < \frac{3}{2}\pi$. When no wake is present the oscillations about the incident field magnitude of unity are greater in the region $\frac{1}{2}\pi < \theta < \pi$ but less in the region $\pi < \theta < \frac{3}{2}\pi$ compared to the case where a wake is present. The diffracted field in the shadow region $-\frac{1}{2}\pi < \theta < 0$ depends strongly on the Mach number,see figure 5 . This field is larger in the leading edge situation (figure 3), than in the trailing edge situation (figure 4). It can be seen that the noise in this region is reduced by the presence of a fluid flow.

Figures 6 and 7 show the far-field for a surface-wave bearing half-plane with $\beta_1 = \beta_2 = -i$. The plot of the still fluid case is not shown as it is identical to figure 4 of Barton and Rawlins [1]. In the leading edge situation (figure 6) the sound level in the shadow region is greater than in the trailing edge situation (figure 7). The reverse situation occurs in the region $\pi/2 < \theta < 3\pi/2$ where the sound level is increased in the trailing edge situation and reduced in the leading edge case.

The situation where the impedance is different on both sides, i.e. the semi-rigid half-plane problem, in the presence of fluid-flow is examined in figures 8-11. The interesting thing we notice is that the effect of lining the upper face of the half-plane produces hardly any difference in the scattered pattern for the trailing (figure 8) and leading edge situation (figure 10). However if the lining is on the lower face of the half-plane there is a considerable difference in the scattered pattern for the trailing(figure 9)and the leading (figure 11) edge situation. It can also be seen from figures 8 and 9 that in the trailing edge situation the field is attenuated more effectively in the shadow region when the half-plane is lined with absorbent material

on the face in the shadow region. From the figures 10 and 11 it can be seen that the field in the shadow region can be greater or smaller depending on the value of θ in the range $-\pi/2 < \theta < 0$, when the lining is on the shadow face. The sound level in the leading(trailing) edge situation is smaller(larger) in the region $-\pi < \theta < -\frac{1}{2}\pi$ when the lining is on the shadow side of the half-plane.

A common feature of all the figures is that the magnitude of the shadow field goes through 0.5 directly below the plate. This result is in fact exactly the same as for the well known Sommerfeld rigid half-plane problem. It has in fact been shown to be an invariant for the impedance half-plane problem, see Rawlins [7]. It looks as if the result is also true for an impedance half plane in a moving fluid.

It is of interest to consider the half-plane as a noise barrier, for example an engine above a wing, and thus to examine the effects of flow to the sound level in the shadow region.It can be seen that the magnitude of the sound diffracted into the shadow region is reduced by the presence of flow in comparison to figures 9 and 11 of Barton and Rawlins [1]. Again, the trailing edge situation is the most efficient for reducing the noise in this region.

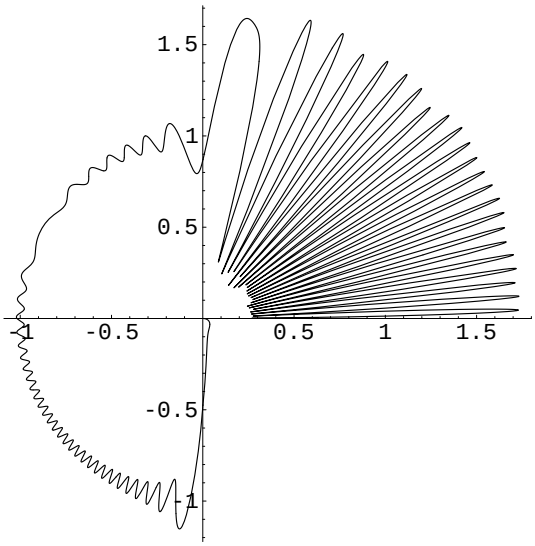

FIGURE 3. $\theta_o = \pi/2$, $\beta_1 = \beta_2 = 0.5 - i$, $M = -0.9$.

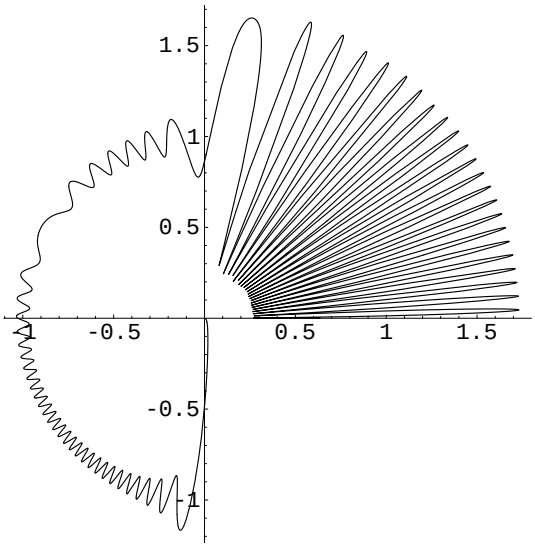

FIGURE 4. $\theta_o = \pi/2$, $\beta_1 = \beta_2 = 0.5 - i$, $M = 0.9$.

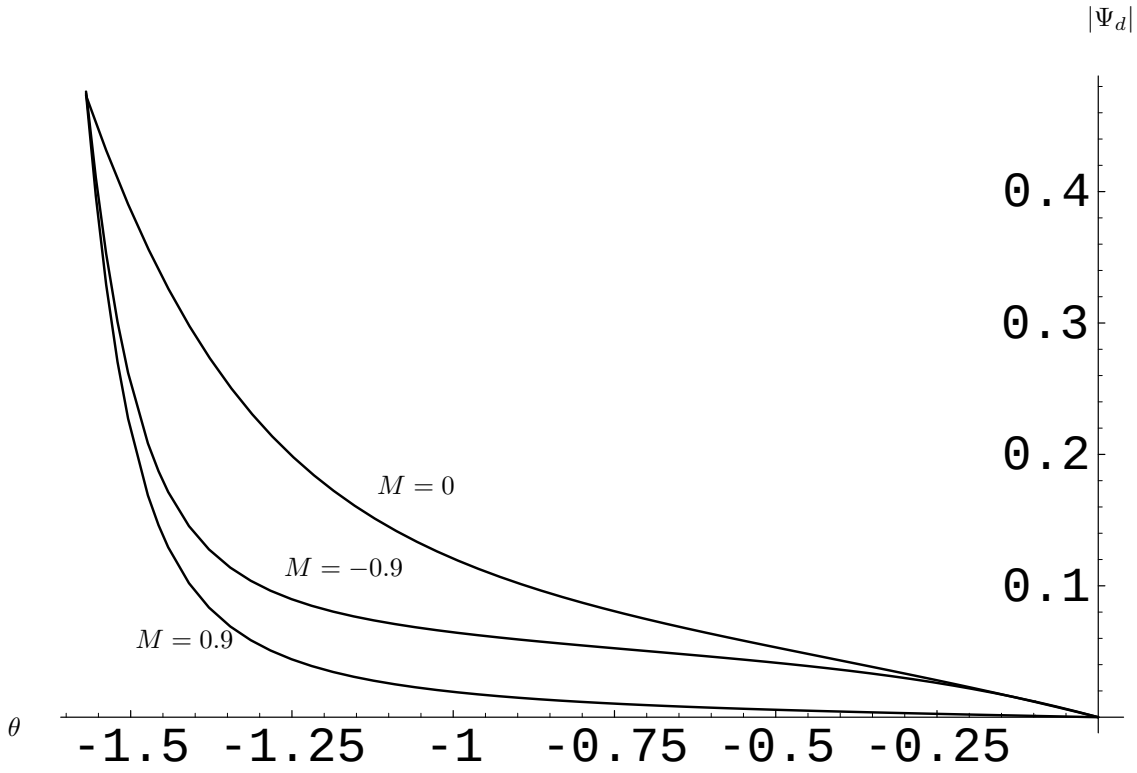

FIGURE 5. The shadow region of a half-plane in a moving fluid, $\beta_1 = \beta_2 = 0.5 - i$.

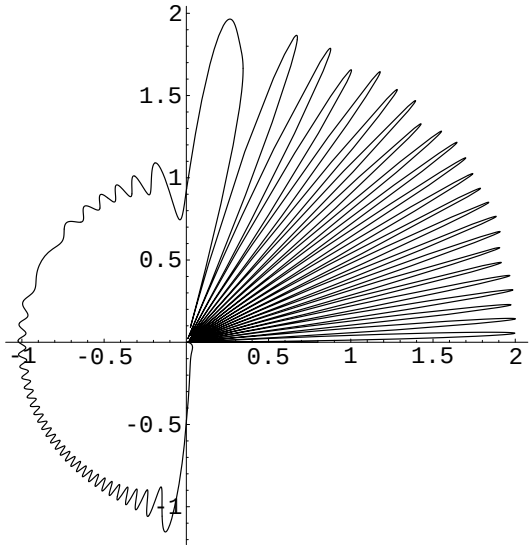

FIGURE 6. $\theta_o = \pi/2$, $\beta_1 = \beta_2 = -i$, $M = -0.9$.

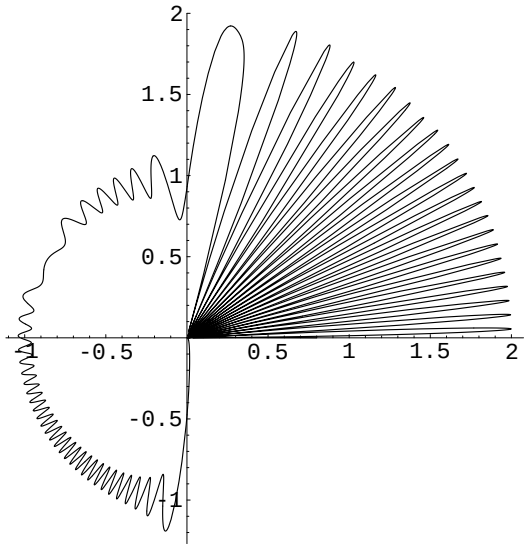

FIGURE 7. $\theta_o = \pi/2$, $\beta_1 = \beta_2 = -i$, $M = 0.9$.

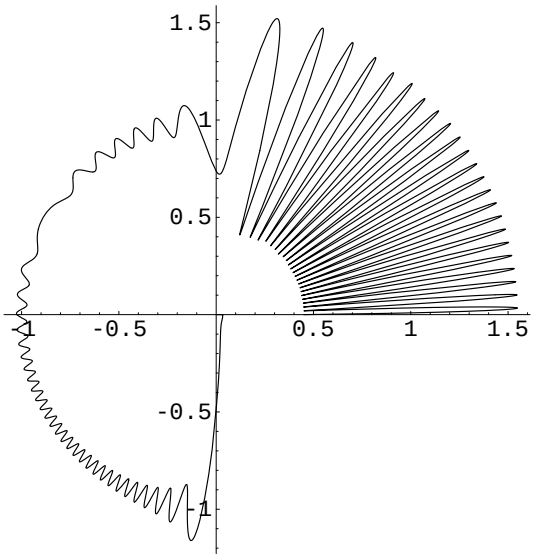

FIGURE 8. $\theta_o = \pi/2$, $\beta_1 = 1.5, \beta_2 = 0$, $M = 0.9$.

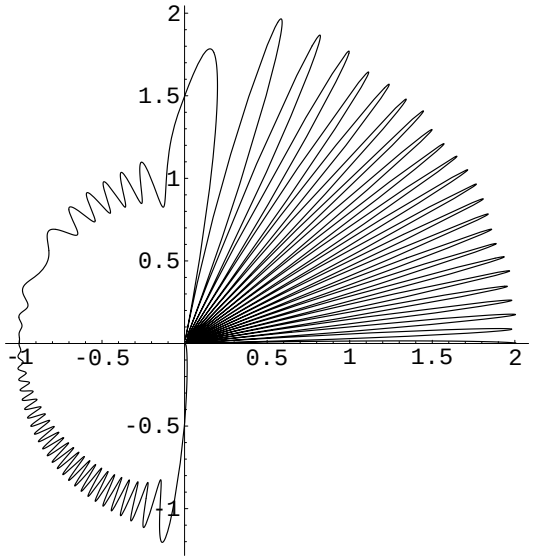

FIGURE 9. $\theta_o = \pi/2$, $\beta_1 = 0, \beta_2 = 1.5$, $M = 0.9$.

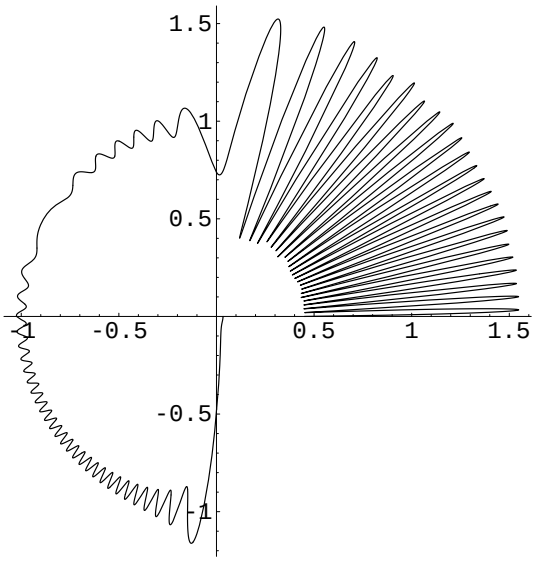

FIGURE 10. $\theta_o = \pi/2$, $\beta_1 = 1.5, \beta_2 = 0$, $M = -0.9$.

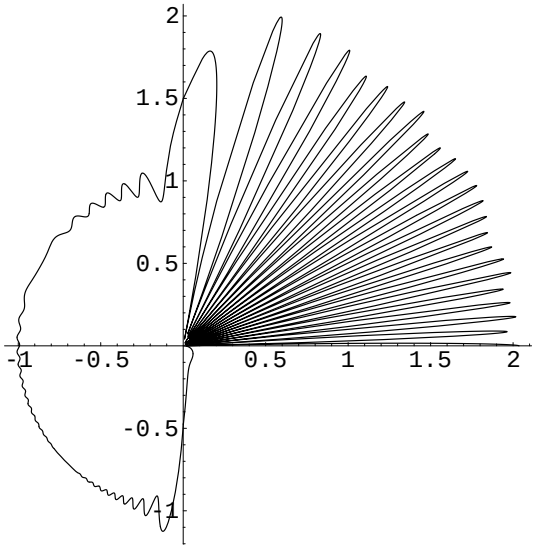

FIGURE 11. $\theta_o = \pi/2$, $\beta_1 = 0, \beta_2 = 1.5$, $M = -0.9$.

8. Conclusions

The problem of a plane wave incident on a half-plane in a moving fluid has been solved without restriction on the impedance parameters of the half-plane. In particular, both absorbent and purely reactive half-planes can be considered with incident plane or surface waves. Moreover, the solution is valid for subsonic values of the Mach number M, and taking $M = 0$ reduces the solution to that of a half-plane in a still fluid.

The solution contains an explicit factorisation of the matrix kernel using the Wiener-Hopf-Hilbert technique. Asymptotic expressions for the far-field were obtained leading to graphical results, which agree with Rawlins [5], and results from Barton and Rawlins [1].

The half-plane in a moving fluid problem has been solved without restriction on β_1 and β_2. Further work could be done therefore on an purely reactive half-plane in a moving fluid. An examination could be carried out on the surface waves arising on the upper and lower surfaces of the half-plane similar to those in Barton and Rawlins [1]. Moreover, results for an incident surface wave can be obtained from the work in this paper.This could lead to substantial sound amplification and possible instabilities in the fluid. A more complicated fluid problem is one where the fluid speed differs in the different halves of the plane. This problem is not solvable by the Maliuzhinets method, which assumes a Sommerfeld integral representation of the field throughout the entire plane. However the present Wiener-Hopf-Hilbert approach offers a possible alternative.

A problem with more practical applications is one of a strip with an absorbent tip in a moving fluid. This would be a model for an aeroplane wing and has the advantage of being cheaper to construct than a strip with faces entirely coated in absorbent materials. Since the problem is governed by the conditions at the diffracting edge, one needs only to consider an absorbent coating in the vicinity of the edge. The present work would act as a first order approximation when the length of the absorbent tip is large, compared to the wavelength of sound.

The results obtained here could also be applied to the problem of the radiation of high frequency sound from a circular cylinder in a moving fluid (see Munt [8]). This is of practical importance as a model of a jet engine in motion. One could investigate noise shielding by examining the effects of lining the cylinder with absorbent materials. To high frequency sound, the edge of the cylinder is locally plane and an application of Keller's geometrical theory of diffraction would give an approximate answer to a mathematically insoluble problem.

Finally this work together with the results of a similar boundary value problem that uses the continuity of particle displacement boundary condition on the absorbent surfaces, will offer useful theoretical comparisons in conjunction with experimental results. This should then lead to a decision as to which is the more appropriate boundary condition to use in practice. Further work in this direction is being currently pursued.

References

[1] P G Barton and A D Rawlins. Acoustic diffraction by a semi-infinite plane with different face impedances. *Q. Jl Mech.appl. Math.* ***52****,1999,469-487.*

[2] A D Rawlins. Acoustic diffraction by an absorbing semi-infinite half plane in a moving fluid. *Proc. R. Soc. Edin. A.* ***72****,1975,337-357.*

[3] A D Rawlins. The solution of a mixed boundary value problem in the theory of diffraction by a semi-infinite plane. *Proc. R. Soc. Lon. A.* ***346****,1975,469-484.*
[4] R A Hurd. The Wiener-Hopf-Hilbert method for diffraction problems.*Can.J.Phys.* ***54****,1976,775-780.*
[5] A D Rawlins.The solution of a mixed boundary value problem in the theory of diffraction.*Jour. Eng. Maths.* ***18****,1984,37-62.*
[6] A H Nayfeh, J E Kaiser and D P Telionis. Acoustics of aircraft engine-duct systems.*AIAA Jl.* ***13****,1975,130-153.*
[7] A D Rawlins. On the optimum orientation of an absorbing barrier. (to appear)*Proc. R. Soc. Lon. A.* ***?****,2005,?-?.*
[8] R M Munt. Acoustic radiation from a circular cylinder in a subsonic stream.*Jl.Inst.Math. Appl.* ***16****,1975,1-10.*
[9] B Noble. Methods based on the Wiener-Hopf technique.*London.Pergamon.1958*
[10] A P Dowling and J E Ffowcs Williams. Sound and sources of sound.*Chichester. Ellis Horwood.1983*

9. Appendix A

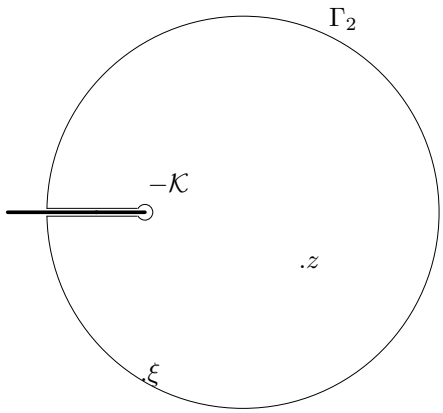

Figure 12. The contour Γ_2 in the complex plane.

Throughout this work the following theorem is required. If $F(z)$ is a holomorphic function of z in $-\pi < arg(z+\mathcal{K}) \leq \pi$; $F(z) = O(z^{-\epsilon})(\epsilon > 0)$ as $|z| \to \infty$ in $-\pi < \arg(z+\mathcal{K}) \leq \pi$ and $F(z)$ satisfies

$$F^+(\xi) - F^-(\xi) = g(\xi), \quad -\infty < \xi < -\mathcal{K},$$

where $g(\xi)$ is a known function then

$$F(z) = \frac{1}{2\pi i}\int_{-\infty}^{-\mathcal{K}} \frac{g(\xi)}{\xi - z} d\xi, \quad -\pi < arg(z+\mathcal{K}) \leq \pi.$$

The proof of this theorem is as follows. For Γ_2 as shown in Figure 12, Cauchy's theorem states that for z inside the contour Γ_2 which is traversed in a positive direction then

$$F(z) = \frac{1}{2\pi i}\int_{\Gamma_2} \frac{F(\xi)}{\xi - z} d\xi.$$

Since $F(z) = O(z^{-\epsilon})$ as $|z| \to \infty (\epsilon > 0)$ the contribution to the above integral from the circular arc is zero. The branch cut contribution gives

$$\begin{aligned} F(z) \quad &= \frac{1}{2\pi i}\int_{-\infty}^{-\mathcal{K}} \frac{F^+(\xi)}{\xi - z} d\xi + \frac{1}{2\pi i}\int_{-\mathcal{K}}^{-\infty} \frac{F^-(\xi)}{\xi - z} d\xi, \\ &= \frac{1}{2\pi i}\int_{-\infty}^{-\mathcal{K}} \frac{F^+(\xi) - F^-(\xi)}{\xi - z} d\xi, \\ &= \frac{1}{2\pi i}\int_{-\infty}^{-\mathcal{K}} \frac{g(\xi)}{\xi - z} d\xi. \end{aligned}$$

10. Appendix B

In this appendix the explicit evaluation of the integrals $I(\alpha)$ and $J(\alpha)$ is given. For the integral

$$I(\alpha) = \int_0^\infty \frac{\log(t+\delta)}{t^{\frac{1}{2}}(t+\gamma)} dt. \tag{60}$$

If it is assumed that γ and δ are real and positive then

$$\begin{aligned} I(\alpha) \quad &= \int_0^\infty \frac{\log|t+\delta|}{t^{\frac{1}{2}}(t+\gamma)} dt, \\ &= 2\int_0^\infty \frac{\log|u^2+\delta|}{u^2+\gamma} du, \\ &= \int_{-\infty}^\infty \frac{\log|u^2+\delta|}{u^2+\gamma} du, \\ &= \int_{-\infty}^\infty \frac{\log|u+i\sqrt{\delta}|}{u^2+\gamma} du + \int_{-\infty}^\infty \frac{\log|u-i\sqrt{\delta}|}{u^2+\gamma} du, \\ &= 2\int_{-\infty}^\infty \frac{\log|u+i\sqrt{\delta}|}{u^2+\gamma} du = 2\mathrm{Re}\int_{-\infty}^\infty \frac{\log(u+i\sqrt{\delta})}{u^2+\gamma} du. \end{aligned}$$

Now consider the integral

$$2\int_\Gamma \frac{\log(z+i\sqrt{\delta})}{z^2+\gamma} dz,$$

where the semicircular closed, positively orientated contour of integration Γ is shown in Figure 13. Using the fact that the contribution from the circular arc is zero and capturing the simple pole at $i\sqrt{\gamma}$ yields

$$2\int_{-\infty}^\infty \frac{\log(u+i\sqrt{\delta})}{u^2+\gamma} du = 2\pi i \lim_{z\to i\sqrt{\gamma}} \frac{\log(z+i\sqrt{\delta})}{z+i\sqrt{\gamma}},$$

$$I(\alpha) = \frac{2\pi}{\sqrt{\gamma}} \log(\sqrt{\gamma}+\sqrt{\delta}), \quad \gamma, \delta > 0. \tag{61}$$

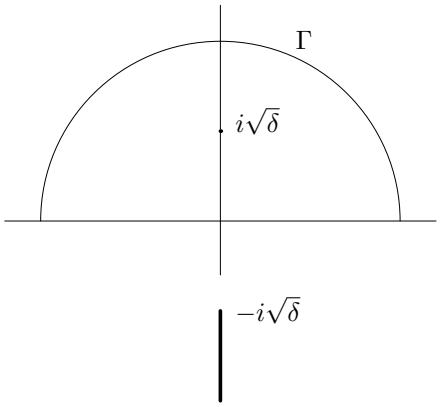

FIGURE 13. Pole capture in the complex plane.

Analytic continuation is now invoked to extend the range of applicability of this result.

$$\int_0^\infty \frac{\log(t+\delta)}{t^{1/2}(t+\gamma)}dt = \frac{2\pi}{\sqrt{\gamma}}\log(\sqrt{\gamma}+\sqrt{\delta}),\ |\arg\gamma|<\pi, |\arg\delta|\le\pi. \tag{62}$$

In Section 3.4 it is also required that

$$\begin{aligned} J(\alpha) \quad &= \int_0^\infty \frac{dt}{t^{1/2}(t+\mathcal{K}+\alpha)}, \\ &= 2\int_0^\infty \frac{du}{u^2+\mathcal{K}+\alpha}, \\ &= \frac{1}{\sqrt{\mathcal{K}+\alpha}}\int_0^\infty \left\{\frac{1}{u+i\sqrt{\mathcal{K}+\alpha}} - \frac{1}{u-i\sqrt{\mathcal{K}+\alpha}}\right\}du, \\ &= \frac{1}{i\sqrt{\mathcal{K}+\alpha}}\left[\log\left(\frac{u-i\sqrt{\gamma}}{u+i\sqrt{\gamma}}\right)\right]_0^\infty, \\ &= \frac{\pi}{\sqrt{\mathcal{K}+\alpha}}. \end{aligned}$$

11. Appendix C

The diffracted field given by expressions (57) and (58) becomes infinite on the boundaries $\Theta = \pi - \Theta_o$ and $\Theta = \pi + \Theta_o$ so an alternate expression has been used to give the graphical plots of the modulus of the far-field. It is noted that Noble [9] gives the following result

$$I = 2i\sin\left(\frac{\Theta_o}{2}\right)\int_{-\infty}^{\infty}\frac{\sin\frac{1}{2}(\Theta+it)e^{i\mathcal{K}R\cosh t}}{\cos(\Theta+it)+\cos\Theta_o}dt = -2iH(\Theta-\Theta_o)+2iH(\Theta+\Theta_o),$$

where

$$H(\lambda) = \begin{cases} \pi^{\frac{1}{2}} e^{-\frac{i\pi}{4}} F\left[\sqrt{2\mathcal{K}R}\cos(\lambda/2)\right] e^{-i\mathcal{K}R\cos\lambda}, & \cos(\lambda/2) > 0, \\ -\pi^{\frac{1}{2}} e^{-\frac{i\pi}{4}} F\left[-\sqrt{2\mathcal{K}R}\cos(\lambda/2)\right] e^{-i\mathcal{K}R\cos\lambda}, & \cos(\lambda/2) < 0, \end{cases}$$

and

$$F[v] = \int_v^\infty e^{iu^2} du.$$

This result, combined with (47) gives the following expression for the diffracted field in the upper half of the plane.

$$\begin{aligned} \Psi_+(R,\Theta) &= \frac{\cos(\Theta/2) u_1[\mathcal{K}\cos\Theta]\{\cos\Theta + \cos\Theta_o\}}{(\mathcal{B}_1 + \mathcal{B}_1 M\cos\Theta + \sin\Theta)\sin(\Theta_o/2)} J_1, && 0 < \Theta < \pi - \Theta_o, \\ &= \frac{\cos(\Theta/2) u_1[\mathcal{K}\cos\Theta]\{\cos\Theta + \cos\Theta_o\}}{(\mathcal{B}_1 + \mathcal{B}_1 M\cos\Theta + \sin\Theta)\sin(\Theta_o/2)}\ J_2, && \pi - \Theta_o < \Theta < \pi. \end{aligned}$$

Where

$$J_1 = 2i\pi^{\frac{1}{2}} e^{-\frac{i\pi}{4}} \Big(e^{-i\mathcal{K}R\cos(\Theta+\Theta_o)} F\left[\sqrt{2\mathcal{K}R}\cos\tfrac{1}{2}(\Theta+\Theta_o)\right] - e^{-i\mathcal{K}R\cos(\Theta-\Theta_o)} F\left[\sqrt{2\mathcal{K}R}\cos\tfrac{1}{2}(\Theta-\Theta_o)\right] \Big),$$

$$J_2 = J_1 - 2\pi i e^{-i\mathcal{K}R\cos(\Theta+\Theta_o)}.$$

Department of Mathematical Sciences, Brunel University, Uxbridge, Middlesex, UB8 3PH, England

E-mail address: Anthony.rawlins@brunel.ac.uk